Retinoic Acid Binds to the C2-Domain of Protein Kinase Cα[†]

Wendy F. Ochoa,[‡] Alejandro Torrecillas,[§] Ignacio Fita,[‡] Nuria Verdaguer,[‡] Senena Corbalán-García,[§] and Juan C. Gomez-Fernandez*[,§]

Instituto de Biología Molecular de Barcelona (CSIC), Jordi Girona Salgado 18-26, E-08034 Barcelona, Spain, and Departamento de Bioquímica y Biología Molecular (A), Facultad de Veterinaria, Universidad de Murcia, Apartado de Correos 4021, E-30080 Murcia, Spain

Received May 2, 2003; Revised Manuscript Received June 5, 2003

ABSTRACT: Protein kinase Cα (PKCα) is a key enzyme regulating the physiology of cells and their growth, differentiation, and apoptosis. PKC activity is known to be modulated by all-*trans* retinoic acid (atRA), although neither the action mechanism nor even the possible binding to PKCs has been established. Crystals of the C2-domain of PKCα, a regulatory module in the protein that binds Ca^{2+} and acidic phospholipids, have now been obtained by cocrystallization with atRA. The crystal structure, refined at 2.0 Å resolution, shows that RA binds to the C2-domain in two locations coincident with the two binding sites previously reported for acidic phospholipids. The first binding site corresponds to the Ca^{2+}-binding pocket, where Ca^{2+} ions mediate the interactions of atRA with the protein, as they do with acidic phospholipids. The second binding site corresponds to the conserved lysine-rich cluster localized in β-strands three and four. These observations are strongly supported by [^{3}H]-atRA-binding experiments combined with site-directed mutagenesis. Wild-type C2-domain binds 2 mol of atRA per mol of protein, while the rate reduces to one in the case of C2-domain variants, in which mutations affect either Ca^{2+} coordination or the integrity of the lysine-rich cluster site. Competition between atRA and acidic phospholipids to bind to PKC is a possible mechanism for modulating PKCα activity.

Protein Kinase C (PKC) is a family of related protein kinases that plays an important role in regulating cell growth as they are involved in several intracellular pathways that end in transcription. PKCs include at least 11 different mammalian isoforms that can be classified into three groups according to their structure and cofactor regulation. The first group includes the classical isoforms (α, βI, βII, and γ) that are regulated by acidic phospholipids, diacylglycerol, phorbol esters, and also by calcium. The second group corresponds to the novel isoforms (δ, ϵ, η, and θ) that are regulated by phospholipids, diacylglycerols, and phorbol esters but not by calcium. The third group comprises the atypical PKC isoforms (ζ, τ/λ, and μ) that are not regulated by diacylglycerol or by calcium (*1*−*3*). PKC isozymes participate in the processes that regulate cell signaling that begin in cell membranes with the appearance of bioactive derivatives of phosholipids such as diacylglycerols (*4*). In particular, classical PKCs are activated by their translocation to membranes in a process regulated by two kinds of molecular signals. The first signal is calcium, which binds to the protein C2-domain that is always present in classical PKCs (*5*), then interacting with the charged groups of anionic phospholipids (*6*). The second signal is diacylglycerol, which binds to the protein C1-domain that, in classical PKCs, occupies the amino-terminal position. Phorbol esters are tumor promoters that also bind to the C1-domains of classical PKCs (*7*).

All C2-domains possess a common fold consisting of an eight-stranded antiparallel β-sandwich with variable loops connecting the strands. In the C2-domains that bind Ca^{2+}, the residues that define the calcium-binding sites form part of the loops on one side of the domain (*6*, *8*). Two or three Ca^{2+} ions were found in the crystal structures of the C2-domains of both PKCβ (*8*) and PKCα (*6*, *9*). In turn, anionic phospholipids have been shown to bind to the C2-domain of PKCα in two different locations, namely, the Ca^{2+}-binding pocket and in the vicinity of the lysine-rich cluster at strands β3 and β4 (*9*).

In the present work, the purified C2-domain of PKCα was cocrystallized with all-*trans* retinoic acid (atRA), and the structure of the complex was determined and refined at 2.0 Å resolution. Retinoids, vitamin A derivatives capable of regulating apoptosis and cellular growth or differentiation, are currently used as therapeutic agents against cancer (*10*−*15*). Empirical data largely support the correlation between the reversion of malignant phenotypes induced by treatment with atRA and the changes in PKC activity. By interacting with nuclear receptors, atRA may control gene expression in tumor cells, and changes in the expression of classical PKCs have been reported for a large variety of cells treated with atRA: F9 embryonal carcinoma cells (*16*), human breast carcinoma cells (*17*, *18*), human pancreatic carcinoma cell lines (*19*), B16 mouse melanoma cells (*20*, *21*), HL-525 (*22*), B16 cells (*23*), and human neuroblastoma cells (*24*). atRA might also affect PKCα activity by altering the localization

[†] This work was supported by the following grants to (a) J.C.G.F. (Universidad de Murcia): BMC2002-00119 from Dirección General de Investigación, Ministerio de Ciencia y Tecnología (Spain) and PI-35/00789/FS/01 from Fundación Séneca (Comunidad Autónoma de Murcia, Spain) and (b) I.F. (Barcelona): BIO099-0865 (Spain).

* To whom correspondence should be addressed. Telephone: +34-968364766. Fax: +34-968364766. E-mail: jcgomez@um.es.

[‡] Instituto de Biología Molecular de Barcelona (CSIC).

[§] Universidad de Murcia.

10.1021/bi034713g CCC: $25.00
Published on Web 07/03/2003

of the protein in the cell, as has been demonstrated to occur in rat splenocytes (*25*) or in human endometrial adenocarcinoma, where redistribution occurs simultaneously with cytoskeletal reorganization (*26*). The reversion of malignancy by treatment with atRA of v-Ki-*Ras*-transformed SVC1 has been associated with both Ras p21 down-regulation and concomitant changes in the cellular localization of PKC (*27*). Finally, it is possible that atRA directly affects the activity of PKCs although little information, either in vitro or in vivo, is available in this respect. Some authors have reported the inhibition of PKC by atRA (*28*−*30*), whereas others found it to be activated (*31*−*32*) or translocated to membranes in vivo (*33*). Even less is known concerning the possible binding of atRA to PKCs, although, on the basis of sequence comparisons with atRA receptors, it has been suggested that atRA might bind close to the Ca^{2+}-binding pocket of the protein C2-domain in classical PKCs (*30*).

Structural results in this work show that RA can interact with the C2-domain in the same two locations that had been previously reported as phospholipid-binding sites (*6*, *9*). One of the sites corresponds to the calcium-binding pocket and the second to the lysine-rich cluster defined by residues at β-strands three and four. These observations are supported by [^{3}H]-atRA-binding experiments combined with site-directed mutagenesis.

MATERIALS AND METHODS

Expression and Purification of the GST-PKC-C2α-Domains. The GST-PKC-C2α wild-type and variants were expressed and purified as described by García-García et al. (*34*) and by Ochoa et al. (*9*), respectively. In summary, the pGEX-KG plasmid containing wild-type or mutant PKC-C2α-domains were transformed into HB 101 *Escherichia coli* cells. The bacterial cultures ($OD_{600} = 0.6$) were induced with 0.2 mM isopropyl 1-thio-β-D-galactopyranoside (IPTG) (Roche) for 6 h at 30 °C. Cells were lysed by sonication in phosphate-buffered saline (PBS) containing protease inhibitors (10 mM benzamidine, 1 mM PMSF, and 10 mL/mL trypsin inhibitor). The soluble fraction of the lysate was incubated with glutathione-Sepharose beads (Pharmacia Biotech, Uppsala, Sweden) for 30 min at 4 °C, which were then washed with PBS three times. Protein concentrations were determined using the method described by Smith et al. (*35*).

Crystallization of PKCα-C2−*Ca^{2+}*−*Retinoic Acid Complex.* The PKCα C2-domain, at 7 mg/mL, was incubated overnight at 4 °C with 25 mM calcium chloride and atRA (Sigma) saturated solution. Crystals were grown using the hanging drop vapor diffusion method with a crystallization medium that contained 20% PEG8000 and 0.05 M potassium phosphate. Crystals were visible after 2−3 days and grew to their maximum size after 4−6 days. These crystals, belonging to space group $P3_221$ with unit cell parameters $a = b = 58.2$ Å and $c = 91.1$ Å were isomorphous to the crystals of PKCα-C2−Ca^{2+} reported previously (*6*), which contained one protein subunit in the asymmetric unit of the crystal (Table 1).

X-ray Data Collection. Structure Determination and Refinement. A single crystal, with approximate dimensions of 0.5 × 0.3 × 0.2 mm and cryo-protected with 20% glycerol, was used to collect a diffraction data set at the temperature of liquid nitrogen with synchrotron radiation at the ESRF (Grenoble) beam line ID14.2. Data evaluation, made with the programs DENZO and SCALEPACK (*36*), gave an internal agreement value R_{sym} of 7.6% with a global completeness of 99% at 2.0 Å resolution (Table 1).

Table 1: Data and Model Refinement Statistics

space group	$P3_221$
cell parameters (Å)	$a = b = 58.2$, $c = 96.1$
resolution range (Å)[a]	20.0−2.0 (2.1−2.0)
unique reflections	12508
R_{sym} (%)[b]	11.3 (44.7)
completeness (%)	99.9 (99.1)
average $I/\sigma(I)$	11.8 (2.6)
R_{work} (%)[c]	23.1
R_{free} (%)[d]	26.4
number of protein residues	135
number of water molecules	72
average thermal factor (Å^2)	
protein	28
water	33
Ca (1/2/3)	26/30/45
RA1[e]	66
RA2	27
PO_4^-	45
geometry deviation	
rmsd Bonds (Å)	0.005
rmsd angles (deg)	1.3

[a] Values in parentheses correspond to the highest resolution shell. [b] $R_{sym} = \sum_{hkl}\sum_i|I_{hkl,i} - \langle I_{hkl}\rangle|/\sum_{hkl}\sum_i I_{hkl,i}$, where $I_{hkl,i}$ is the observed intensity and $-\langle I_{hkl}\rangle$ is the average intensity of multiple observations of symmetry-related reflections. [c] $R_{work} = \sum_{hkl}||F_{obs}| - |F_{calc}||/\sum_{hkl}|F_{obs}|$, where F_{obs} and F_{calc} are the observed and calculated structure factors, respectively. [d] R_{free} has the same definition as R_{work} for a cross-validation set of about 5% of the reflections. [e] RA1 is located in the calcium-binding region, and only the acidic moiety of the molecule has been modeled (see text). RA2 is located in the vicinity of the lysine-rich cluster region.

The structure was solved by molecular replacement with the AMoRe program using as a searching model the structure of the PKCαC2−Ca^{2+} complex (*6*) with Ca^{2+} ions and solvent molecules excluded (*37*). The correctly oriented and positioned model yielded a correlation coefficient of 60% and an *R*-factor of 35% for data in the resolution shell from 15 to 3.5 Å. Iterative positional and temperature refinement with CNS (*38*), including bulk solvent correction, was alternated with manual rebuilding using the interactive graphic program O (*39*) with difference and omit ($2F_o - F_c$) and ($F_o - F_c$) electron density maps.

Refinement of the ternary PKCα-C2−Ca^{2+}−RA complex, at 2.0 Å resolution, converged with the crystallographic agreement factors R_{work} and R_{free} of 23.1 and 26.4%, respectively. The final model comprises 135 protein residues, from Thr156 to Pro291, 72 well-ordered water molecules, three Ca^{2+} and one phosphate ion, and two RA molecules, one of them modeled only partially (Figure 1 and Table 1). The structure exhibits good stereochemistry with all the residues situated within the most favorable or permitted regions of the Ramachandran plot (*40*). Coordinates are deposited in the Protein Data Bank and are also available on request from the authors.

Binding Measurements. A standard assay contained 20 μg of the PKC-C2α-domain bound to 20 μL of glutathione-Sepharose beads. Beads were prewashed with the binding buffer containing 50 mM Hepes pH 7.4, 100 mM NaCl, and 200 μM $CaCl_2$. The different solutions were prepared in the

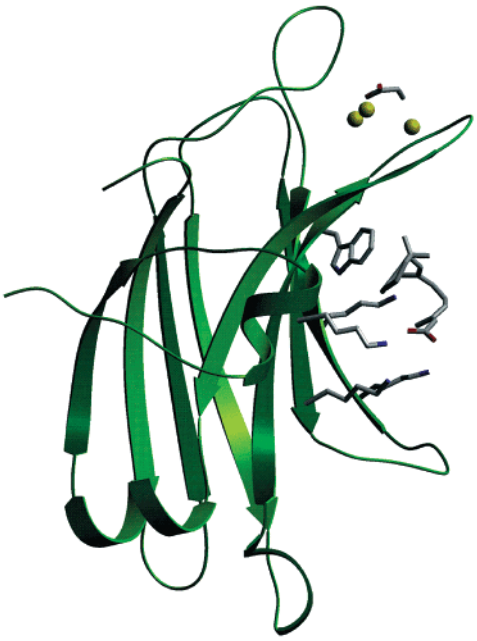

FIGURE 1: Overall ribbon representation of the PKCαC2−Ca^{2+}−RA structure. Calcium ions are represented as green spheres, while the RA molecules and the phosphate group are indicated as solid sticks. Protein residues in the lysine-rich cluster site are also explicitly shown.

same binding buffer with [11,12-^{3}H(N)] atRA (approximately 25 000 cpm/nmol). A total of 50 μL of the solutions were added to the beads. The mixture was incubated at room temperature for 30 min with vigorous shaking and then briefly centrifuged in a tabletop centrifuge. The beads were washed twice with 200 μL of the binding buffer without atRA. Binding was quantified by liquid scintillation counting of the beads. Additional control binding experiments were performed using GST bound to glutathione-Sepharose beads so that data were corrected for nonspecific binding. Data represent the means of triplicate determinations (±SD).

RESULTS AND DISCUSSION

Overall Structure. The PKCα-C2-domain from rat, including residues from His155 to Gly293, was produced as a recombinant fragment and crystallized in the presence of Ca^{2+} and atRA. The quality of the final electron density map enabled the position of most residue side chains to be established accurately and confirmed the presence of the ternary complex (PKCα-C2−Ca^{2+}−RA) in the crystal. The structure showed the presence of three Ca^{2+} ions at the calcium-binding pocket (Figure 2), the positions of which corresponded to these previously termed as Ca1, Ca2, and Ca3 in some PKCα-C2-domain complexes (*9*) that, in turn, were equivalent to the three calcium sites found in the structure of PKCβ-C2 (*8*). A putative phosphate group, which simultaneously bound to Ca2 and Ca3, has also been included in the final model, again similarly to that reported in the PKCαC2−Ca^{2+}−DAPS complex (*9*). A density in the Ca^{2+}-binding site close to Ca1 was interpreted as corresponding to a partially ordered atRA molecule (Figure 2). A well-defined and continuous extra electron density, with a horseshoe shape, was also found in the lysine-rich cluster region at strands β3 and β4, and this density was assigned to a second RA-binding site (Figure 3A).

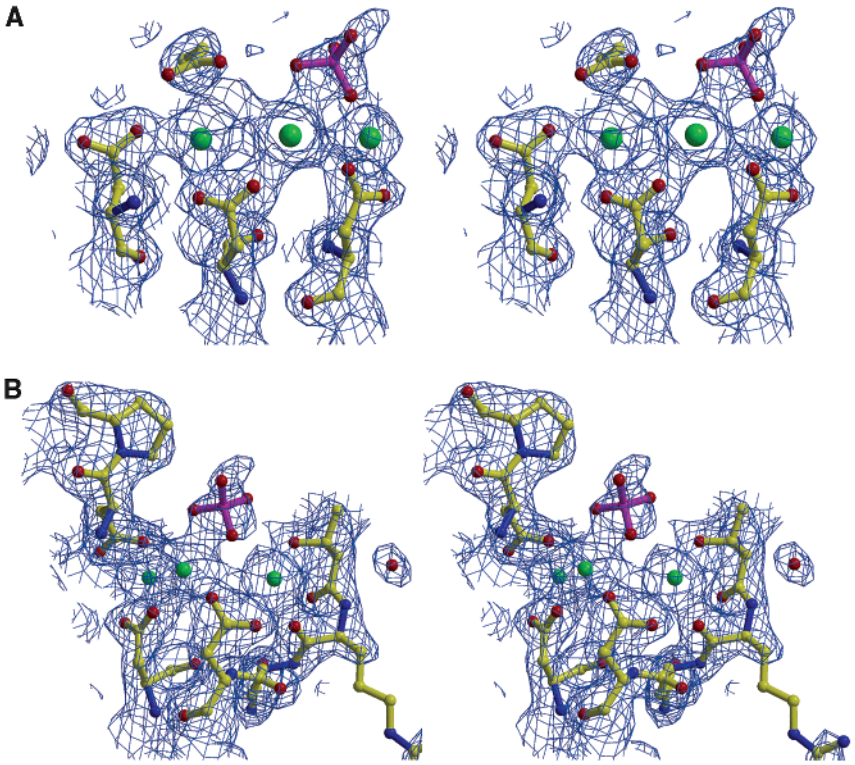

FIGURE 2: Stereoviews, 90° apart from each other, of the final ($2F_o - F_c$) electron density map in the calcium-binding pocket. Electron density is displayed with a chicken-box representation. Calcium ions are represented as green spheres. The putative phosphate group (pink) and the RA molecule fragments are also explicitly depicted. For clarity, only aspartic residues 193, 246, and 254 are shown in panel A. In turn, residues Pro188, Thr251, and Arg252 have also been added to better define the environment around Ca3 in panel B. The Arg252 side chain has been found to be disordered in all the PKCαC2-domain structures determined to date.

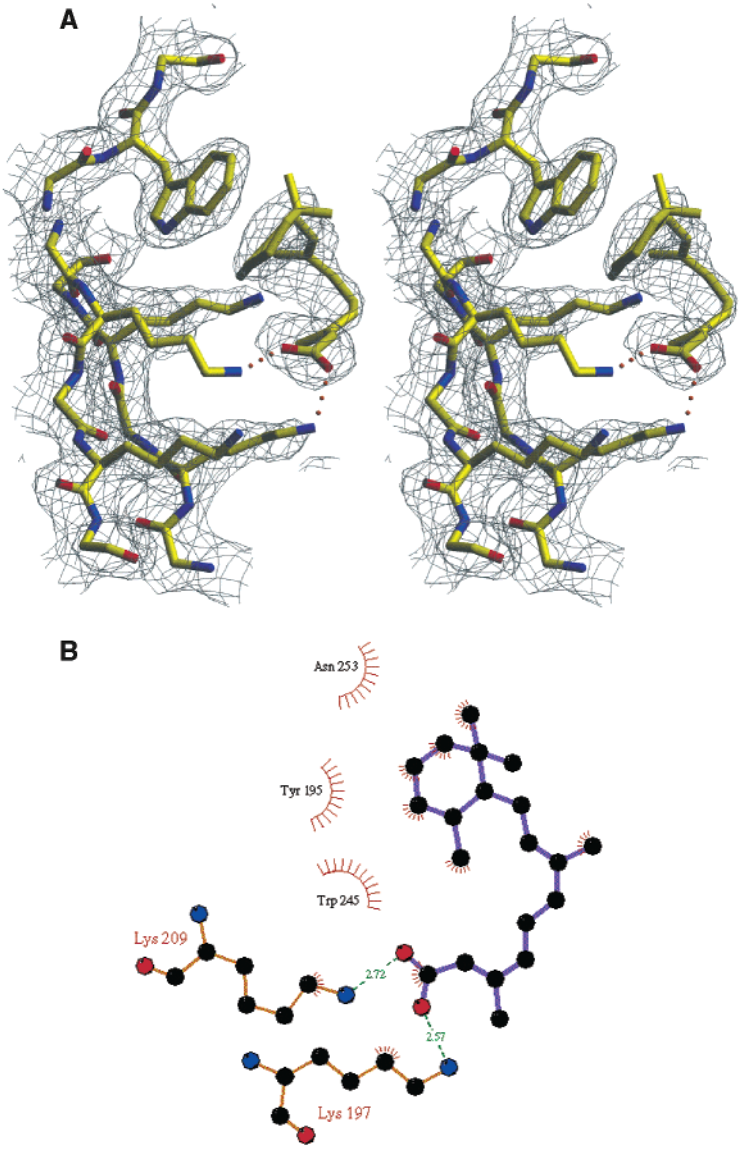

FIGURE 3: (A) Stereoview of the final ($2F_o - F_c$) electron density map in the vicinity of the lysine-rich cluster site. The RA molecule shown has been modeled as an 11-cis isomer (see text). (B) LIGPLOT (*48*) depicting the interactions of the RA molecule, modeled in the lysine-rich cluster site, with residues from the C2-domain.

The root-mean-square deviation (rmsd) resulting from the superimposition of C^{α} atoms from the PKCα-C2−Ca^{2+}−RA and PKCα-C2−Ca^{2+} complexes is only 0.12 Å, with most side chains in similar positions in both structures. Therefore, no significant rearrangement of the structure of the C2-domain in the presence of calcium seemed to be required to bind RA.

Calcium-Binding Pocket. The three Ca^{2+} ions found in locations equivalent to the calcium sites Ca1, Ca2, and Ca3 (*9*) have temperature factors of 26, 30, and 45 $Å^2$, respectively (Table 1). Ca1 and Ca2 show hepta coordination with side chain oxygen atoms from five Asp residues (187, 193, 246, 248, and 254) and the main chain oxygen atoms of residues Met186 and Trp147 (*6*, *9*). In turn, Ca3 is hexa coordinated with side chain oxygen atoms from Asp248, Thr251, Asp254, and with the main chain oxygen of Arg252 (*9*). The remaining extra electron density in the calcium-binding pocket region was interpreted as being due to poorly ordered atRA molecules and a phosphate ion. The density in the vicinity of Ca1 had sufficient continuity for it to be modeled as an acid group with the first few carbon atoms of an atRA molecule (Figure 2A). This atRA molecule is situated in the same location as was occupied by a phospholipid in the structures of the PKCα-C2−Ca^{2+}−phospholipid complexes (*6*, *9*). The acid group of this RA molecule completes the coordination sphere of Ca1, while the aliphatic portion presents a number of hydrophobic interactions with residues from the C2-domain loops CBR1 and CBR3, in particular, the aliphatic part of Arg249. Extra density in the vicinity of both Ca2 and Ca3 is located close to the site where a phosphate ion is found in the PKCα-C2−Ca^{2+}−DAPS structure (*9*), and a phosphate has been maintained in the present model despite its nearness to the Pro188 side chain (Figure 2B). Therefore, RA binding to the calcium-binding pocket seems to be dominated by electrostatic interactions that directly bridge the RA acid moieties to the calcium ions. Hydrophobic interactions may also contribute but are so unspecified that the aliphatic portion of the RA molecule appears to be mostly disordered. A similar interaction pattern has already been observed for the PKCα-C2-domain when

interacting with acidic phospholipids (*6*, *9*).

Whereas some authors reported the inhibition of PKC by atRA (*28*−*30*), others, as indicated above, observed activation (*31*, *32*) or translocation to membranes in vivo (*33*). These apparently contradictory reports might now be reconciled by the observation that atRA can replace the phospholipid in the calcium-binding pocket. With atRA participating in the anchoring of PKC to membranes when Ca^{2+} is present, it is possible to envisage that atRA would induce activity even in the absence of specific phospholipids (*31*) and that the effect on PKC activity would vary depending on the relative concentrations of Ca^{2+}, atRA, and phospholipids.

Lysine-Rich Cluster Site. Extra electron density in the lysine-rich cluster region indicated the presence of a second RA-binding site in the C2-domain (Figure 3A). This binding site is situated in the same location and was found to be occupied by a phospholipid in the structures of PKCα-C2−Ca^{2+} with DCPA and with DAPS, respectively (*9*). When an RA molecule is modeled inside this dense zone, both the carboxylic group and the aliphatic ring ends of the molecule interact with the C2-domain. The carboxylic group establishes electrostatic bonds with side chains from lysine residues 197, the only one in the cluster with poor electron density, and 209. These electrostatic interactions and the residues involved are closely equivalent to those seen between the C2-domain and the corresponding phospholipid in the complexes with both DCPA and DAPS. In turn, the aliphatic ring presents a number of hydrophobic interactions, mainly with residues Tyr195 and Trp245 (Figure 3B). However, a strong curvature of the density was observed, and it is not clear whether the conformation is still all-trans, although strong bending of atRA molecules when bound to a retinoic acid-binding protein have already been reported (*41*). However, it is not possible to exclude that this appearance corresponds to a strong disordering of the retinoic acid molecule or even to the presence of an isomer different from the all-trans.

The role of the lysine-rich cluster has been investigated in PKCs by mutational analysis (*42*, *43*), but no changes were found in enzymatic activity. However, binding of phosphatidylserine and also of phosphatidic acid in the lysine-rich cluster region has been observed in the crystal structures of the C2-domain complexes from PKC α (*9*), and additionally, *o*-phospho-L-serine has been observed to bind with the C2-domain from PKC β (*8*). In fact, mutational studies also showed that, in the absence of Ca^{2+}, the binding of the domain to phospholipid membranes was reduced with respect to the wild-type (*9*). It appears that when Ca^{2+} is present, the calcium-binding pocket will determine the binding to membranes, and only when Ca^{2+} is absent will the contribution of the cluster to binding become apparent. We suggest that even in the presence of Ca^{2+}, the lysine-rich cluster may be important for the proper positioning of the enzyme with respect to the membrane and that this cluster may also be involved in the tethering of the C2-domain with the C1A-domain in the inactive conformation of the enzyme (*9*). The liberation of this lysine cluster from the site to which diacylglycerol binds may be one of the key activation steps of the enzyme (*9*). In addition, through the mutation of two lysine residues (K209 and K211) located in this lysine-rich cluster, it has been demonstrated that these are key residues in the PtdIns(4,5)P_2-driven activation process of PKC α (*44*). Therefore, the capacity of atRA to occupy the lysine-rich cluster-binding site may also have important implications in the modulation of PKC activity.

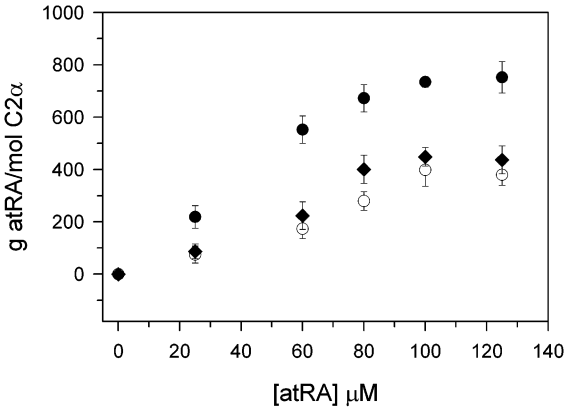

FIGURE 4: Binding of [11,12-^{3}H(N)] all-*trans* retinoic acid to the C2-domain of PKCα. The protein was bound to gluthatione-Sepharose beads. Wild-type protein (●) is compared to two mutants: D246/248N (○) and K197/209/211A (◆). Ratios of grams of atRA per mol of C2 protein are plotted against micromolar concentrations of atRA.

[^{3}H]-Retinoic Acid Binding Assay to C2-Domain. Binding experiments, performed at increasing concentrations of [^{3}H]-atRA (Figure 4), show that saturation was reached at about 800 g of atRA/mol of protein and given that the molecular weight of atRA is 400.3, this means that saturation is at 2 mol of atRA per mole of C2 protein, in close agreement with the structural results. Note that half saturation will be reached in this case, at about 40 μM atRA, and this gives us an idea that the affinity of C2 for atRA site-directed mutagenesis in the C2-domain was also carried out to change some of the key residues in the two binding sites where the retinoic acid molecules were found. For the double mutant Asp246Asn/Asp248Asn, saturation was reached at about 450 g/mol, which means 1.13 mol of atRA/mol C2 protein (Figure 4). It had been previously shown that this double mutant lacks, almost totally, Ca^{2+}-binding capacity, and its enzymatic PKC activity is greatly inhibited (*45*, *46*). This means that the half saturation is reached in this case at about 65 μM atRA, so that the affinity is considerably reduced in comparison with the wild protein. The triple mutant Lys197Ala/Lys209Ala/Lys211Ala, in the lysine-rich cluster, reached saturation binding at about 390 g of atRA/mol of C2 and this means 0.98 mol of atRA/mol of C2 protein (Figure 4). In this case, half saturation is again reached at about 58 μM indicating again a reduction in affinity with respect to the wild protein. These experiments clearly suggest then that one atRA molecule binds at the Ca^{2+}-binding site and another one at the lysine-rich site, and the data are compatible with a similar affinity for atRA of both sites.

CONCLUSION

Binding of atRA to the C2-domain of PKCα had been proposed on the basis of sequence comparisons with other retinoic acid binding proteins (*30*). In these predictions, binding sites had been approximately defined as situated in the PKCα region between residues 240−280, which includes some of the C2-domain residues in the calcium-binding pocket. Results from the present work confirm binding of

RA to the C2-domain of PKCα. Binding takes place in the same two locations that had been described as binding sites of acidic phospholipids, namely, at the Ca^{2+}-binding pocket and in the vicinity of the lysine-rich cluster (*9*). It is clear that PKCα can act, at least in vitro, as an RA receptor. The observed competition between phospholipids and RAs for the same binding sites immediately suggests a way to modulate PKCα activity that could be related with the proven capacity of atRA to revert malignant phenotypes (*20*, *24*, *47*). Additional in vivo studies are needed to precisely calibrate the physiological and pharmacological implications of the findings reported in this paper.

ACKNOWLEDGMENT

We wish to thank to Drs. Ono and Nishizuka for the kind gift of cDNA encoding PKCα. We thank Dr. P. Zamora-Conesa for his help in some preliminary experiments.

REFERENCES

1. Nishizuka, Y. (1995) *FASEB J. 9*, 484−496.
2. Mellor, H., and Parker, P. J. (1998) *Biochem. J. 332*, 281−292.
3. Newton, A. C. (2001) *Chem. Rev. 101*, 2353−2364.
4. Nishizuka, Y. (1992) *Science 258*, 607−614.
5. Coussens, L., Parker, P. J., Rhee, L., Yang-Feng, T. L., Chen, E., Waterfield, M. D., Francke, U., and Ullrich., A. (1986) *Science 233*, 859−866.
6. Verdaguer, N., Corbalán-García, S., Ochoa, W. F., Fita, I., and Gómez-Fernández, J. C. (1999) *EMBO J. 18*, 6329−6338.
7. Kikkawa, U., Takai, Y., Miyake, R., and Nishizuka, Y. (1983) *J. Biol. Chem. 258*, 11442−11445.
8. Sutton, R. B., and Sprang, S. R. (1998) *Structure 6*, 1395−1405.
9. Ochoa, W. F., Corbalán-García, S., Eritja, R., Rodríguez-Alfaro, J. A., Gómez-Fernández, J. C., Fita, I., and Verdaguer, N. (2002) *J. Mol. Biol. 320*, 277−291.
10. Wang, Z. Y., and Chen, Z. (2000) *Lancet Oncol. 1*, 101−106.
11. Altucci, L., and Gronemeyer, H. (2001) *Nature Rev. Cancer 1*, 181−193.
12. Sun, S. Y., and Lotan, R. (2002) *Crit. Rev. Oncol. Hematol. 41*, 41−55.
13. Douer, D. (2002) *Acta Haematol. 107*, 1−17.
14. Fontana, J. A., and Rishi, A. K. (2002) *Leukemia 16*, 463−472.
15. Hozumi, M. (1998) *Int. J. Hematol. 68*, 107−129.
16. Cho, Y., Klein, M. G., and Talmage, D. A. (1998) *Cell Growth Differ. 9*, 147−154.
17. Cho, Y., Tighe, A. P., and Talmage, D. A. (1997) *J. Cell Physiol. 172*, 306−313.
18. Cho, Y., and Talmage, D. A (2001) *Exp. Cell Res. 269*, 97−108.
19. Rosewicz, S., Brembeck, F., Kaiser, A., Marschall, Z. V., and Riecken, E. O. (1996) *Endocrinology 137*, 3340−3347.
20. Gruber, J. R., Desai, S., Blusztajn, J. K., and Niles, R. M. (1995) *Exp. Cell Res. 221*, 377−384.
21. G. Boskovic, D., Desai, S., and Niles, R. M (2002) *J. Biol. Chem. 277*, 26113−26119.
22. Yang, K. D., Mizobuchi, T., Kharbanda, S. M., Datta, R., Huberman, E., Kufe, D. W., and Stone, R. M. (1994) *Blood 83*, 490−496.
23. Desai, D. S., Hirai, S., Karnes, W. E., Jr., Niles, R. M., and Ohno, S. (1999) *Biochem. Biophys. Res. Commun. 263*, 28−34.
24. Tonini, G. P., Parodi, M. T., Di Martino, D., and Varesio, L. (1991) *FEBS Lett. 280*, 221−224.
25. Hozumi, M. (1998) *Int. J. Hematol. 68*, 107−129.
26. Carter, C. A., Parham, G. P., and Chambers, T. (1998) *Pathobiology 66*, 284−292.
27. Spina, A., Chiosi, A. E., Naviglio, S., Pagano, M., Illiano, G., Marchese, M., Spena, S. R., Buommino, E., Morelli, F., and Metáfora, S. (2000) *Biochim. Biophys. Acta 1496*, 285−295.
28. Cope, F. O., Staller, J. M., Mahsem, R. A., and Boutwell, R. K. (1984) *Biochem. Biophys. Res. Commun. 120*, 593−601.
29. Cope, F. O., Howard, B. D., and Boutwell, R. K. (1986) *Experientia 42*, 1023−1027.
30. Radominska-Pandya, A., Chen, G., Czernik, P. J., Little, J. M., Samokyszyn, V. M., Carter, C. A., and Nowak, G. (2000) *J. Biol. Chem. 29*, 22324−22330.
31. Ohkubo, S., Yamada, E., Endo, T., Itoh, H., and Hidaka, H. (1984) *Biochem. Biophys. Res. Commun. 118*, 460−466.
32. Bouzinba-Segard, H., Fan, X. T., Perderiset, M., and Castagna, M. (1994) *Biochem. Biophys. Res. Commun. 204*, 112−118.
33. Zorn, N. E., and Sauro, M. D. (1995) *Int. J. Immunopharmacol. 17*, 303−311.
34. García-García, J., Corbalán-García, S., and Gómez-Fernández, J. C. (1999) *Biochemistry 38*, 9667−9675.
35. Smith, P. K., Krohn, R. I., Hermanson, G. T., Mallia, A. K., Gartner, F. H., Provenzano, M. D., Fujimoto, E. K., Goeke, N. M., Olson, B. J., and Klenk, D. C. (1985) *Anal. Biochem. 150*, 76−85.
36. Otwinowski, Z. (1993) Oscillation data reduction program, in *Proceedings of the CCP4 Study Weekend: Data Collection and Processing* (Sawyer, L., Isaacs, N., and Bailey, S., Eds.) pp 56−62, SERC Daresbury Laboratory, Warrington, England.
37. Navaza, J. (1994) *Acta Crystallogr. A50*, 157−163.
38. Brünger, A. T., Adams, P. D., Clore, G. M., DeLano, W. L., Gros, P., Grosse-Kunstleve, R. W., Jiang, J. S., Kuszewski, J., Nilges, M., Pannu, N. S. et al. (1998) *Acta Crystallogr. D54*, 905−921.
39. Jones, T. A., Zou, J. Y., Cowan, S., and Kjeldgaard, M. (1991) *Acta Cryst. A47*, 110−119.
40. Laskowski, R. A., MacArthur, M. W., Moss, D. S., and Thornton, J. M. (1993) *J. Appl. Crystallogr. 26*, 283−291.
41. Newcomer, M. E., Pappas, R. S., and Ong, D. E. (1993) *Proc. Natl. Acad. Sci. U.S.A. 90*, 9223−9227.
42. Edwards, A. S., and Newton, A. C. (1997) *Biochemistry 36*, 15615−15623.
43. Jonhson, J. E., Edwards, A. S., and Newton, A. C. (1997) *J. Biol. Chem. 272*, 30787−30792.
44. Corbalán-García, S., García-García, J., Rodríguez-Alfaro, J. A., and Gómez-Fernández, J. C. (2002) *J. Biol. Chem. 278*, 4972−4980.
45. Corbalán-García, S., Rodríguez-Alfaro, J. A., and Gómez-Fernández, J. C. (1999) *Biochem. J. 357*, 513−521.
46. Conesa-Zamora, P., Gómez-Fernández, J. C., and Corbalán-García, S. (2000) *Biochim. Biophys. Acta 1487*, 246−254.
47. Kahl-Rainer, P., and Marian, B. (1994) *Nutr. Cancer. 21*, 157−168.
48. Wallace, A. C., Laskowski, R. A., and Thornton, J. M. (1995) *Protein Eng. 8*, 127−134.

BI034713G